# Supporting Information

## Carbon Nanofiber @ ZIF-8 Derived Carbon Nanosheets Composites with Core-shell Structure Boosting Capacitive Deionization Performance

Xinyi Gong‡, Wanxia Luo‡, Nannan Guo, Su Zhang, Luxiang Wang*, Dianzeng Jia*, Lili Ai, and Shizhan Feng

State Key Laboratory of Chemistry and Utilization of Carbon Based Energy Resources; Key Laboratory of Advanced Functional Materials, Autonomous Region; Institute of Applied Chemistry, College of Chemistry, Xinjiang University, Urumqi, 830046, Xinjiang, PR China.

Corresponding author E-mail: wangluxiangxju@163.com (L. Wang)

‡ These authors contributed equally to this work.

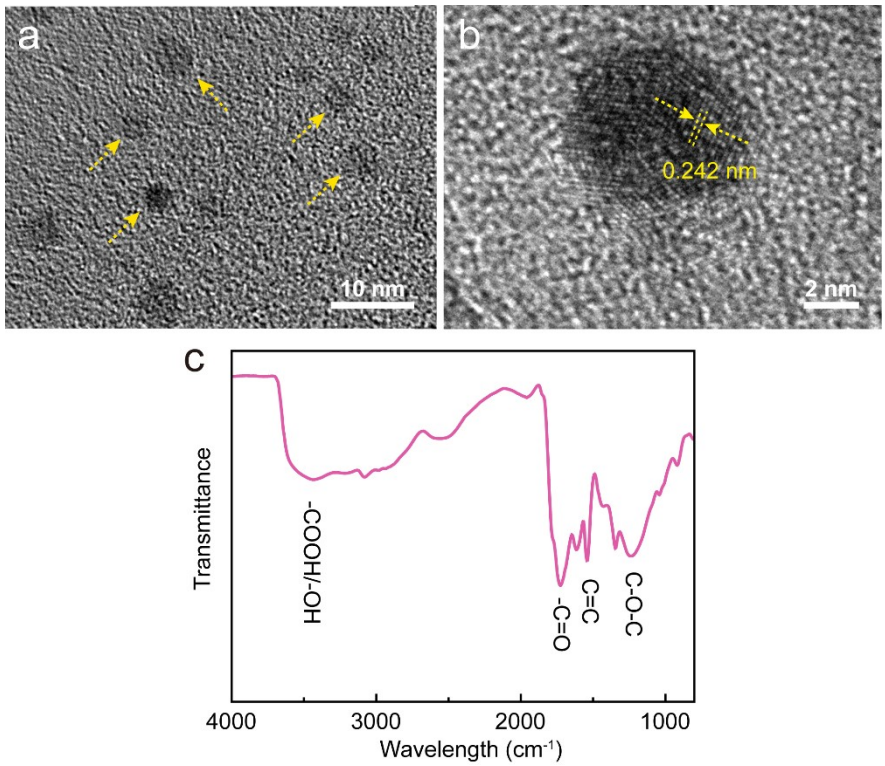


**Figure S1.** (a) Low-magnification and (b) high-resolution TEM images of graphene quantum dots, (c) FT-IR spectrum of graphene quantum dots.

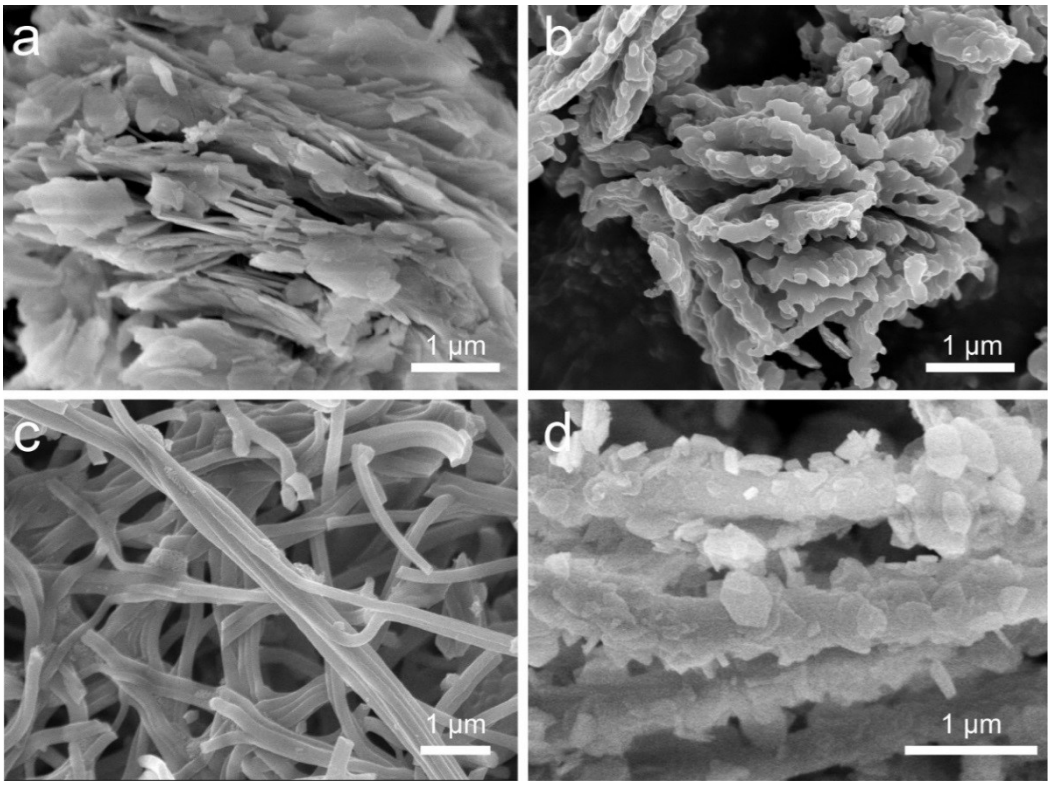


**Figure S2.** SEM images of ZIF-8 nanosheets (a) before and (b) after carbonization ($C_{ZIF}$), (c) $PAN_{ZIF\text{-}10}$, and (d) $P\text{-}CNF_{ZIF\text{-}10}$.

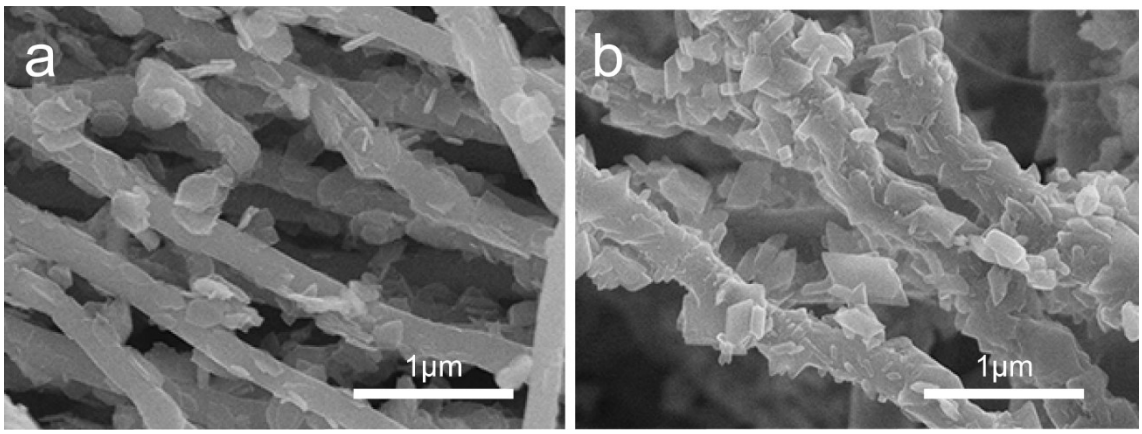


**Figure S3.** SEM images of (a) $CNF_{ZIF-5}$ and (b) $CNF_{ZIF-15}$.

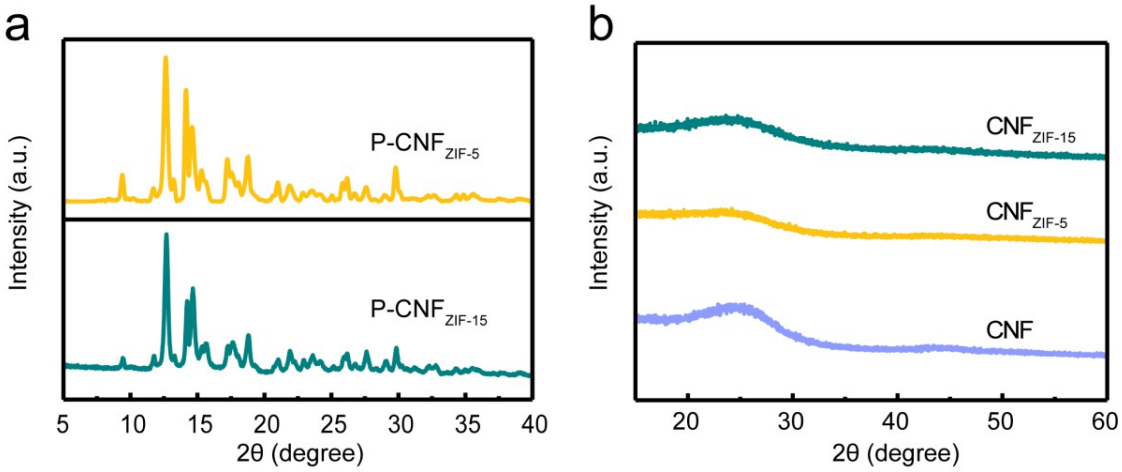


**Figure S4.** The XRD patterns of (a) P-$CNF_{ZIF-X}$ and (b) CNF and $CNF_{ZIF-X}$.

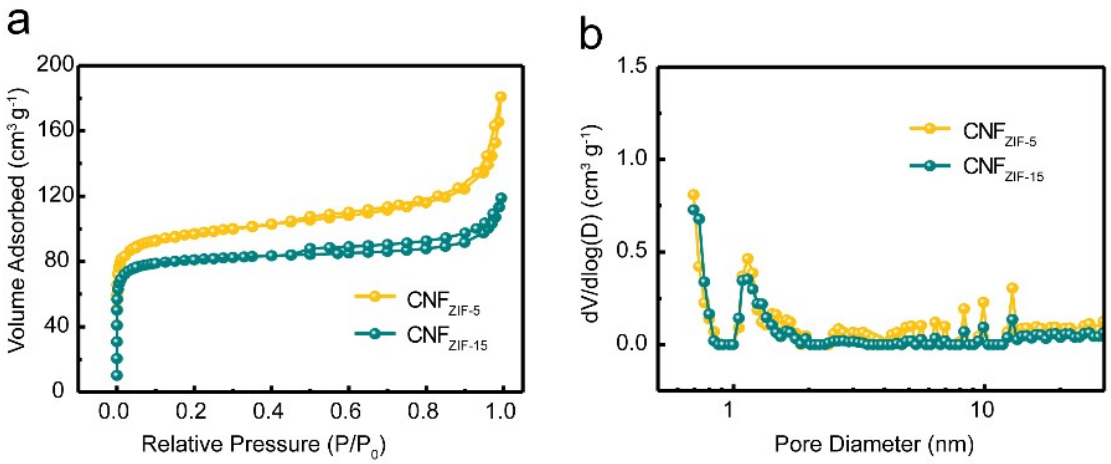


**Figure S5.** (a) $N_2$ adsorption-desorption isotherms and (b) pore size distribution of $CNF_{ZIF-5}$ and $CNF_{ZIF-15}$.

**Table S1** Texture properties derived from $N_2$ adsorption-desorption isotherms.

| Sample | $S_{BET}$[a] ($m^2\ g^{-1}$) | $V_{total}$[b] ($cm^3\ g^{-1}$) | $V_{meso}$[c] ($cm^3\ g^{-1}$) | $V_{micro}$[d] ($cm^3\ g^{-1}$) |
|---|---|---|---|---|
| CNF | 244 | 0.146 | 0.035 | 0.111 |
| $CNF_{ZIF-5}$ | 358 | 0.209 | 0.095 | 0.114 |
| $CNF_{ZIF-10}$ | 416 | 0.215 | 0.075 | 0.140 |
| $CNF_{ZIF-15}$ | 276 | 0.157 | 0.044 | 0.113 |

[a] Specific surface area calculated by BET method.

[b] Total pore volume .

[c] Volume of mesopores.

[d] Volume of micropores by t-plot method.

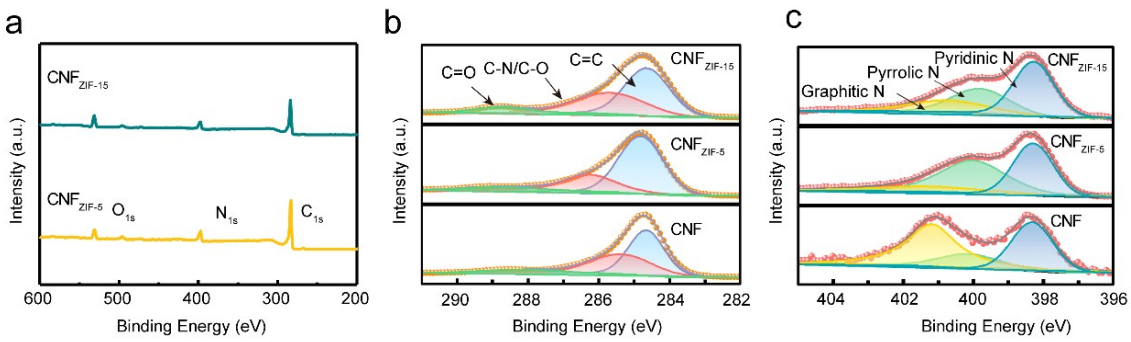


**Figure S6.** (a) XPS survey spectra of $CNF_{ZIF-5}$ and $CNF_{ZIF-15}$; (b) $C_{1s}$ and (c) $N_{1s}$ XPS spectra of CNF, $CNF_{ZIF-5}$, and $CNF_{ZIF-15}$.

**Table S2** Surface composition of the samples derived from XPS analysis (in atomic %)

| Sample | C | N | O | Pyridinic N | Pyrrolic N | Graphitic N |
|---|---|---|---|---|---|---|
| CNF | 82.4 | 6.9 | 10.7 | 27.5 | 12.2 | 60.3 |
| $CNF_{ZIF-5}$ | 80.1 | 12.8 | 7.1 | 37.4 | 47.1 | 15.5 |
| $CNF_{ZIF-10}$ | 79.5 | 13.0 | 7.5 | 39.9 | 39.6 | 20.5 |
| $CNF_{ZIF-15}$ | 75.3 | 13.1 | 11.6 | 50.7 | 32.3 | 17.0 |

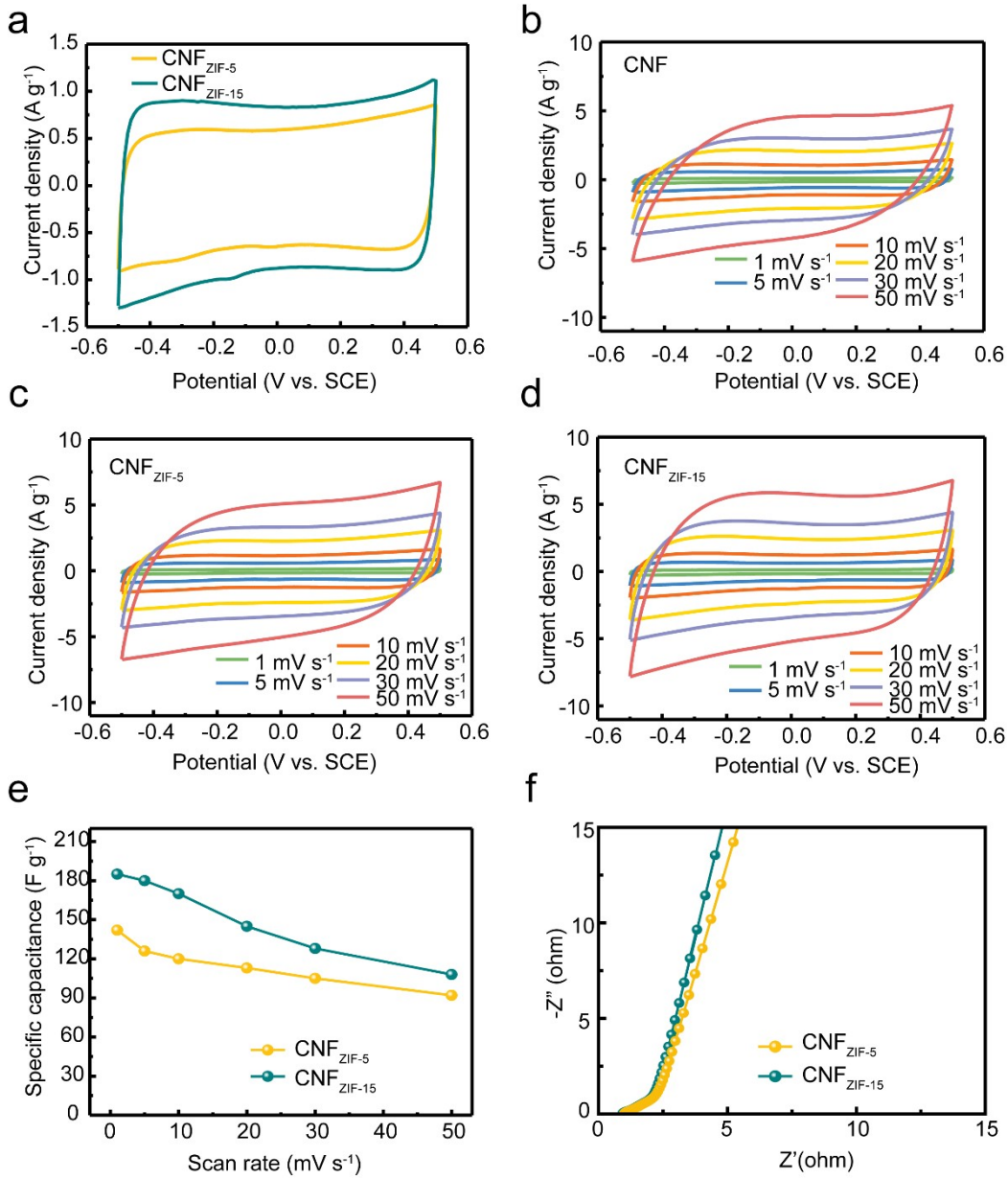


**Figure S7.** (a) CV curves of $CNF_{ZIF-5}$ and $CNF_{ZIF-15}$ at 5 mV $s^{-1}$; (b) CV curves of CNF, (c) $CNF_{ZIF-5}$, and (d) $CNF_{ZIF-15}$ at different scan rates. (e) specific capacitance versus scan rate and (f) Nyquist plots of $CNF_{ZIF-5}$ and $CNF_{ZIF-15}$.

**Table S3** The $R_{ct}$ values of $C_{ZIF}$, CNF, and $CNF_{ZIF-X}$ electrodes.

| Samples | $C_{ZIF}$ | CNF | $CNF_{ZIF-5}$ | $CNF_{ZIF-10}$ | $CNF_{ZIF-15}$ |
|---|---|---|---|---|---|
| $R_{ct}$ (Ω) | 0.27 | 1.27 | 0.24 | 0.11 | 0.20 |

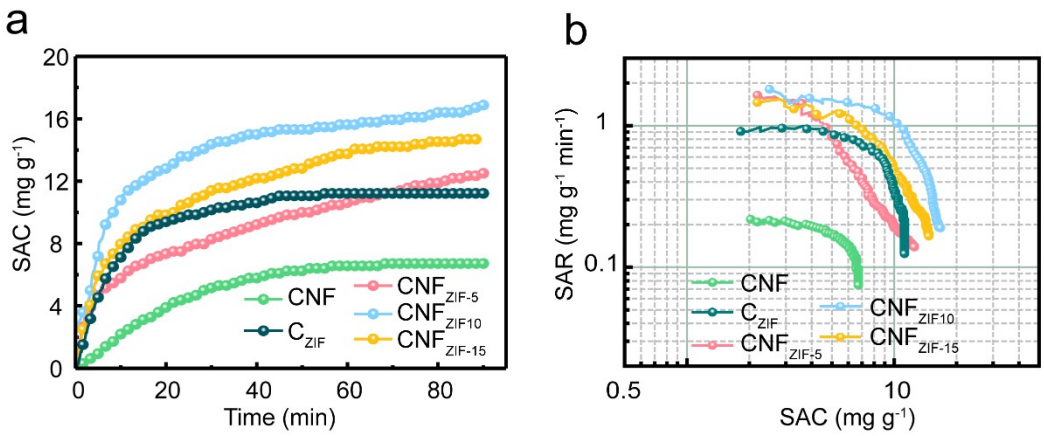


**Figure S8.** (a)The SAC curves and (b) CDI Ragone plots of CNF, $CNF_{ZIF-X}$, and $C_{ZIF}$ in a 500 mg $L^{-1}$ NaCl solution.

**Table S4** Comparison of the CDI performance of various electrode materials in a NaCl solution.

| Sample | Initial concentration ($mg\ L^{-1}$) | Voltage (V) | SAC ($mg\ g^{-1}$) | Ref. |
|---|---|---|---|---|
| mGE | 500 | 1.2 | 14.2 | **S1** |
| N-HMCSs | 500 | 1.2 | 16.6 | **S2** |
| PCN6 | 1000 | 1.2 | 16.26 | **S3** |
| ZIF-67/CNT | ~300 | 1.2 | 10.3 | **S4** |
| ECAG | ~87 | 1.8 | 14.25 | **S5** |
| PCS | 500 | 1.2 | 10.3 | **S6** |
| PCP1200 | 500 | 1.2 | 13.89 | **S7** |
| GR/NMC | 500 | 1.2 | 14.5 | **S8** |
| SCZs | 500 | 1.2 | 15.31 | **S9** |
| MOF/PPy | 500 | 1.2 | 11.34 | **S10** |
| | 100 | | 8.59 | |
| $CNF_{ZIF-10}$ | 500 | 1.2 | 16.89 | **This work** |
| | 800 | | 19.69 | |

**References**:


S1. X. Xu, Y. Liu, M. Wang, X. Yang, C. Zhu, T. Lu, R. Zhao and L. Pan, *Electrochim. Acta*, 2016, **188**, 406-413.

S2. Y. Li, J. Qi, J. Li, J. Shen, Y. Liu, X. Sun, J. Shen, W. Han and L. Wang, *ACS Sustain. Chem. Eng.*, 2017, **5**, 6635-6644.

S3. T. Lu, Y. Liu, X. Xu, L. Pan, A. A. Alothman, J. Shapter, Y. Wang and Y. Yamauchi, *Sep. Purif. Technol.*, 2020, **256**, 117771.

S4. X. Xu, C. Li, C. Wang, L. Ji, Y. V. Kaneti, H. Huang, T. Yang, K. C. W. Wu and Y. Yamauchi, *ACS Sustain. Chem. Eng.*, 2019, **7**, 13949-13954.

S5. M. S. Zoromba, M. H. Abdel-Aziz, M. Bassyouni, S. Gutub, D. Demko and A. Abdelkader, *ACS Sustain. Chem. Eng.*, 2017, **5**, 4573-4581.

S6. Y. Li, X. Xu, S. Hou, J. Ma, T. Lu, J. Wang, Y. Yao and L. Pan, *Chem. Commun.*, 2018, **54**, 14009-14012.

S7. Y. Liu, X. Xu, M. Wang, T. Lu, Z. Sun and L. Pan, *Chem. Commun.*, 2015, **51**, 12020-12023.

S8. T. Yan, J. Liu, H. Lei, L. Shi, Z. An, H. S. Park and D. Zhang, *Environ. Sci. Nano:*, 2018, **5**, 2722-2730.
S9. J. Shen, Y. Li, C. Wang, R. Luo, J. Li, X. Sun, J. Shen, W. Han and L. Wang, *Electrochim. Acta*, 2018, **273**, 34-42.
S10. Z. Wang, X. Xu, J. Kim, V. Malgras, R. Mo, C. Li, Y. Lin, H. Tan, J. Tang, L. Pan, Y. Bando, T. Yang and Y. Yamauchi, *Mater. Horizons*, 2019, **6**, 1433-1437.